Article
Performance Validation of PM Assisted SynRM and PMSM with Optimized Design for EV Application

Swapnil Jani[1],* , and Jitendra Jamnani[2]

1   Nirma University, Ahmedabad, Gujarat, India.
2   Pandit Deendayal Energy University, Department of Electrical Engineering, Gandhinagar, India
*   Correspondence: swapnil.jani@nirmauni.ac.in

Abstract: This paper presents the comparison of Permanent Magnet-Assisted Synchronous Reluctance Motor (PMASynRM) and Permanent Magnet Synchronous Motor (PMSM) for the same design parameters and the evaluation of various performance parameters based on the Finite Element (FE) Method. FE Analysis is conducted after selecting the optimized design for PMASynRM and PMSM using an FE tool, with loading conditions to determine various performance parameters. This is achieved by maintaining the same motor dimensions and stator parameters while altering the rotor geometry for both motors. The final simulation results are discussed, and other performance parameters are recorded for comparison purposes. A PMASynRM is introduced, in which the problems of Synchronous Reluctance Motor (SynRM) can be eliminated with a permanent magnet in the rotor flux barrier. Due to higher flux barriers in PMASynRM, the reluctance torque is higher than in PMSM. If the magnet is placed very near to the air gap in PMSM, higher magnet torque is achieved, but due to the high reluctance torque in PMASynRM, the electromagnetic torque of PMASynRM is higher compared to PMSM. The research proves that the proposed design of PMASynRM is the best choice for Electric Vehicle (EV) applications. For PMASynRM, the shape of the flux barrier is not possible to change due to the design limitation of the FE software tool. Further analysis can be conducted by changing the shapes of the flux barriers to propose the most effective barriers. Basic theory and FE analysis of conventional PMSM and SynRM are reported in the literature. An optimal design is proposed through comparative analysis for EV applications to find out the best candidate for an EV motor.

1. Introduction

Generally, Permanent Magnet Brushless DC motors (PMBLDC) for 2-wheeler Electric Vehicle (EV) applications, Surface Mounted Permanent Magnet (SPM) motors, Interior Permanent Magnet (IPM) motors, and Switched Reluctance motors have been used for EVs [1–3]. For four-wheeler applications, Permanent

Magnet Synchronous Motors (PMSMs) and Induction Motors (IM) are the preferred choice. Among these motors, PMSM is the best candidate due to its higher power density, improved Power Factor (PF), and greater efficiency. Hence, PMSMs are widely used by EV manufacturing industries [4–6].

PMSM is the best choice due to its high Constant Power Speed Range (CPSR) and superior technical features, but it has some limitations, such as demagnetization at higher temperatures, a narrow constant power region, and high cost due to the presence of Permanent Magnets (PMs). In contrast, by using PM-assisted Synchronous Reluctance Motor (PMASynRM), the performance of the motor is improved compared to the conventional Synchronous Reluctance Motor (SynRM), making it suitable for use in both EVs and Hybrid Electric Vehicles (HEV) with minor limitations [7–9]. Furthermore, the availability of rare earth magnets, their high cost, and fluctuating rates are significant issues for PMSMs. In PMASynRMs, reluctance torque is the dominant component, and by adding PMs in lesser composition in the flux barriers, performance can be improved similarly to PMSMs. This will increase the CPSR of PMASynRM. Very few researchers have focused on the comparative analysis of PMSM and PMASynRM for electric vehicular applications. Comparisons were made based on PM volume, torque, inductances, and flux linkages for low-power motors [10–13].

In this paper, basic theory, phasor diagrams, and analytical design equations for PMSMs and PMASynRMs are presented. Based on requirements, design parameters for PMSMs and PMASynRMs are selected, and accordingly, optimized designs are performed through Finite Element (FE) software. For the same design specifications, the first Finite Element Analysis (FEA) of PMSMs is conducted with Interior PMSMs (IPMSMs). The selection of IPMSMs is made because this motor is used in EVs, which require high CPSR and better PM employment in rotor geometry [14, 15]. The performance of IPMSMs is drastically affected by different rotor geometries [16–18]. The selection of suitable rotor geometry depends on higher CPSR, high torque, better mechanical strength, reliability at high speed, and ease of manufacturing. Here, the V-shape PM motor is selected [19–21]. For PMASynRMs, eight rotor poles are selected with four flux barriers per pole, and FE analysis is conducted. Due to the addition of PMs, issues like torque ripple and cogging torque are present in PMASynRMs, but various techniques in the literature can minimize these issues. However, this paper does not focus on these issues [22, 23].

After the introduction, this paper is organized as follows: fundamental theory concepts of motors are discussed to choose the final design parameters; the methodology of FEA is elucidated and discussed. In the next part, plots of various motor parameters are recorded and analyzed. Furthermore, waveforms of different performance parameters are captured and investigated for PMSMs and PMASynRMs. Results are compared for PMSMs and PMASynRMs, and concluding remarks are presented in the last section of the paper.

2. Theory of PMASynRM

Figure 1, stator and rotor structure of synchronous reluctance motor and PM-assisted synchronous reluctance motor are shown. To achieve the maximum power density in reluctance motors, d-axis inductance must be high with respect to q-axis inductance. The ratio of L_d and L_q is defined as the saliency ratio. The problem with synchronous reluctance motor is L_q is high due to the reluctance of air presented in flux barriers, while in PM-assisted SynRM, by adding the PMs to the flux barriers, q-axis current is reduced due to PM saturation and hence inductance of q-axis is minimal. So, the saliency ratio is increased and so, the power density of PMASynRM is increased, which is desirable for EV applications. In Figure 2(a), an equivalent circuit of a motor is presented with machine voltage and current, reluctance, and inductance. In Figure 2(b), the same concept, due to the addition of PMs, how the vectors are affected is mentioned with vectorial representation [6].
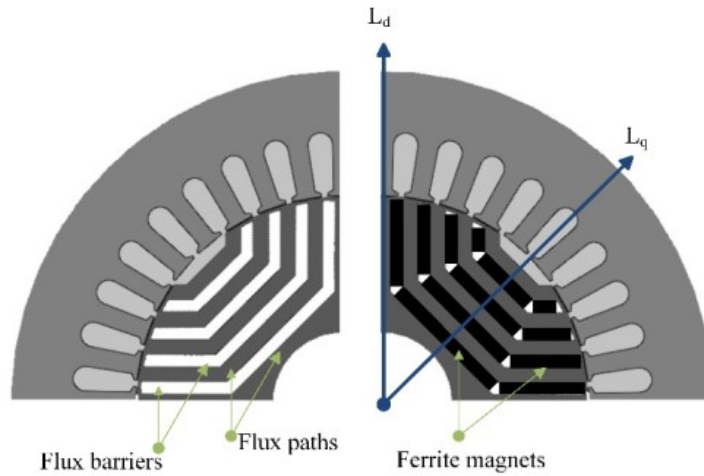
Figure 1. The sketch of SynRM (left side) and PMSynRM (right side) stator and rotor structure.

The PMASynRM offers commendable performance at high speeds, satisfying the constant-power speed range requirements. If EV manufacturers requirement is to develop the low-cost solution against PMSM, the use of ferrite magnets provides consistent solution. Another attractive advantage of PMASynRM is it has improved power factor compared to conventional SynRM due to the high flux linkage because of PMs insertion in flux barriers. This will also help to reduce the VA rating of inverter, which will further reduce the size of power drive-train [24].
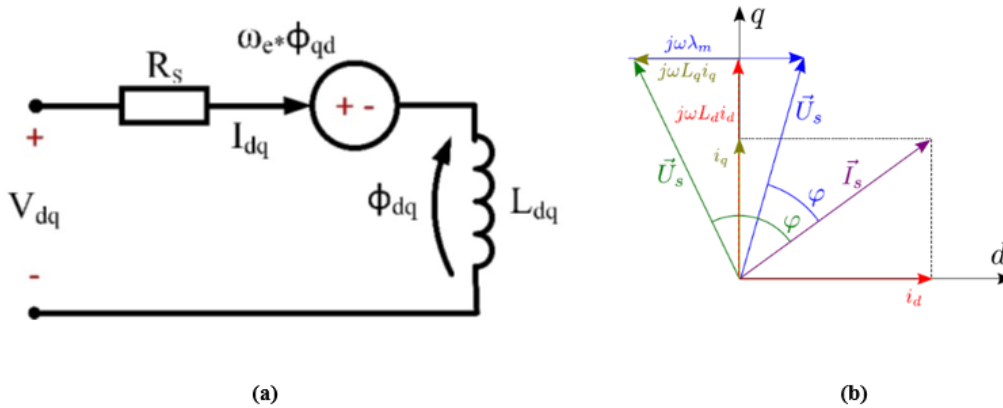

Figure 2. (a) Equivalent Circuit and (b) Phasor diagram of PMSM and PMASynRM.

3. Finite Element Design Methodology for PMASynRM and PMSM

For the proposed FE analysis of PMASynRM and PMSM, first geometries as per the design specifications are drawn. Afterwards, type of analysis, model and element is selected. In the preprocessing part, suitable materials of different parts of the motor i.e., stator, rotor, back iron, magnet, conductors etc. Subsequently for more accurate analysis, meshing of the geometry is carried out. In next step, after applying proper load, model is solved and various performance parameters are recorded. This is the generalize process for both motors which is represented in Figure 3.

Every analysis involves four main steps:

- Preliminary Decisions
  - Which analysis type?
  - What to model?
  - Which element type?
- Pre processing
  - Define Material
  - Create or import the model geometry
  - Mesh the geometry
- Solution
  - Apply loads
  - Solve
- Post processing
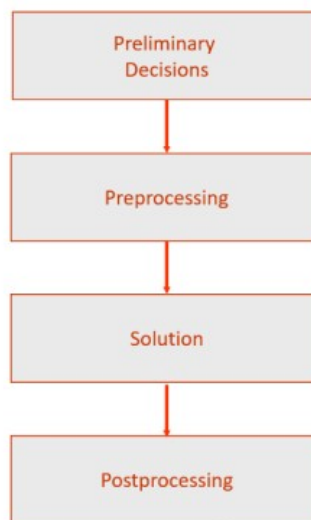 - Review results
  - Check the validity of the solution

Figure 3. Finite element analysis procedure of PMASynRM.

Table 1. Design Parameters/Specification of PMASYNRM (Stator Parameters).

Stator Parameter	Dimensions
Stator Diameter	269.24 mm
Stator Bore	161.9 mm
Slot Width (Bottom)	8 mm
Slot Width (Top)	5 mm
Slot Depth	35 mm
Slot Corner radius	2.5 mm
Tooth Tip depth	0.2 mm
Slot Opening	1 mm
Tooth Tip Angle	20°
Sleeve Thickness	0 mm

For the analysis purpose, for PMASynRM, design with 48 number of semi enclosed stator slots is selected with 3-phase ac distributed winding as shown in Figure 4(a). In stator winding, heavy stator slot is built with 24 stranded conductors per stator slot, overlapping divider and wedge model is selected. For the rotor winding, eight number of rotor poles are selected with 1 mm airgap. In this analysis, NdFeB (1.39 T), are selected for FE analysis. The laminated sheet steel with low grade is used for the stator, while for rotor core high saturation flux density material (high grade silicon steel) is preferred to reduce core losses. FE analysis is done by considering the 150 A current (RMS), 200 V DC bus voltage and 3000 rpm speed. Flux density distribution is depicted in Figure 5(a) for PMASynRM. In Figure 6 and Figure 7, current and voltage waveforms are displayed. For this PMASynRM, 08 rotor poles are chosen with 04 number for flub barriers per pole. This helps to increase the permanent magnet torque component in the total electromagnetic torque of motor. PMs inner magnet length in decreasing from shaft to stator side in all geometries. This will help to reduce the requirement of PM materials in each flux barriers as well as cost of PMs and also to increase the flux linkage. Less volume of PMs is also helpful to get the torque with less torque ripple. Design specifications of PMASynRM for FE analysis are tabulated in Table 1 and Table 2.

The main goal of this research work is to compare the performance of PMASynRM and PMSM for the same frame size and main motor dimensions for EV application. Rated parameters and loading condition

Table 2. Design Parameters/Specification of PMASynRM (Rotor Parameters).

Rotor Parameter	Dimensions	Rotor Parameter	Dimensions
L1 Diameter	80 mm	L1 Inner Mag Length	10
L1 Bridge Thickness	0.8 mm	L1 Inner Mag Segments	1
L1 Web Thickness	8 mm	L1 Inner Mag Offset	0
L1 Outer Angle Offset	0	L1 Inner Mag gap I	0
L1 Outer Thickness	3 mm	L1 Inner Mag gap O	0
L1 Outer Mag Length	0	L1 Inner Post	0
L1 Outer Mag Segments	1 mm	L1 Inner Post offset	0
L1 Outer Mag Offset	0	L1 Central Post	0
L1 Outer Mag gap I	0	Rotor poles	4
L1 Outer Mag gap O	0	Mag Layers (Barriers)	2
L1 Outer Post	0	Airgap	1
L1 Outer Post offset	0	Shaft Diameter	40
L1 Inner Thickness	4	Shaft Hole Diameter	10

Table 3. Design Parameters of PMSM (Rotor).

Rotor Parameter	Dimensions	Rotor Parameter	Dimensions
L1 Magnet Thickness	4 mm	L1 Magnet Post	0.1 mm
L1 Magnet V Width	22 mm	L1 Magnet Segments	1
L1 Magnet Shift	0 mm	L1 Mag Gap Inner	0
L1 Magnet Bar Width	22 mm	L1 Mag Gap Outer	0
L1 Bridge Thickness	2 mm	Airgap	1 mm
L1 Pole V Angle	130 °	Banding Thickness	0
L1 Outer Extension	2 mm	Shaft Diameter	80 mm
L1 Inner Extension	2 mm	Shaft Hole Diameter	10 mm
L1 Outer Mag gap I	0	Rotor poles	4
L1 Outer Mag gap O	0	Mag Layers (Barriers)	2
L1 Outer Post	0	Airgap	1
L1 Outer Post offset	0	Shaft Diameter	40
L1 Inner Thickness	4	Shaft Hole Diameter	10

are also kept same for the precise comparison. Internal structure, rotor geometry and materials might be change by designer based on the requirements and accommodation of PM flux barriers in given space. Motor parameters are kept identical for healthier comparison. For PMSM, stator structure is same as PMASynRM as discussed earlier. The selection of rotor structure for PMSM is very important. There are various rotor topologies for PMSM are investigated and reported in literature [11, 12]. Hence V-type of rotor structure is selected as shown in Figure 4(b), which can effectively utilize the PM excitation compare to conventional straight type PM rotor structure of IPMSM. Hence to determine the PM thickness, PM width and V-type angle between to PMs of V-type rotor are key requirement. In this paper, PMSM is design with suitable optimal motor parameters including stator and rotor geometry, airgap, PM in flux barriers by using FEM tool ANSYS MOTOR CAD. The quantity of PMs in V-type rotor core, highly influence the performance parameters of PMSM. For this analysis, NdFeB (1.39 T) is considered as magnet material due to its superior magnetic properties. Flux density distribution is depicted in Figure 5(b) for PMSM. Although, cost and availability issued are faced by NdFeB, but for this proposed work these factors are not important to be covered. Researchers have already made conclusions based on the investigation in this regard, hence this part is not included here. Design specifications of rotor for FE analysis for PMSM

are tabulated in Table 3. Stator dimensions are kept same as PMASynRM for the PMSM FE analysis. To compare the performance of PMASynRM and PMSM geometries are simulated by applying 3D solver of ANSYS MOTOR CAD.

Figure 4. (a) PMASynRM with 08 rotor poles and 04 flux barriers, (b) PMSM with 08 rotor poles and 04 flux barriers.
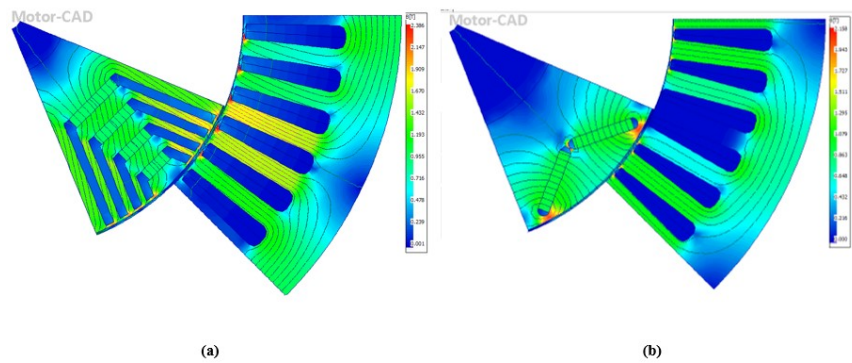

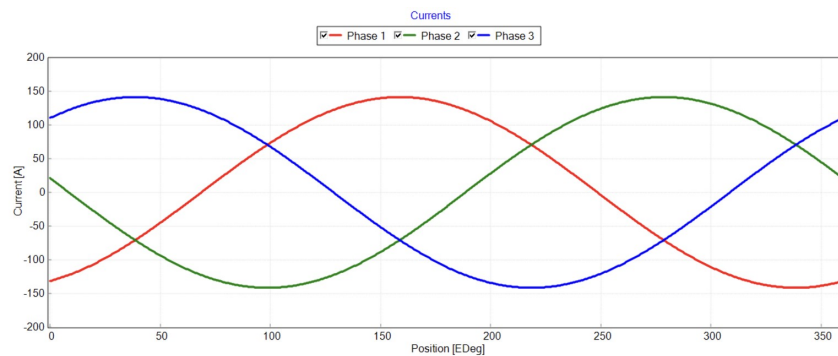**Figure 5.** (a) Flux Density distribution for PMASynRM, (b) Flux Density Distribution for PMSM.

Figure 6. Input Current Waveform.

4. Comparison and analysis of performance parameters of PMASynRM and PMSM

FE analysis is done based on the given machine parameters and satisfactory results are obtained for various performance parameters for both the motors as per the mentioned design specifications. With this
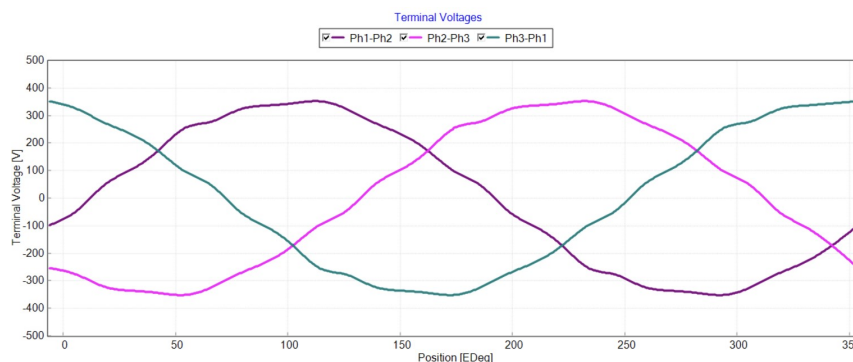
Figure 7. Terminal Voltage Waveform.

proposed topology of PMASynRM and PMSM, back emf waveforms were obtained as per Figure 8 and Figure 9. This is sufficient to produce the required amount of electromagnetic torque in the motor.
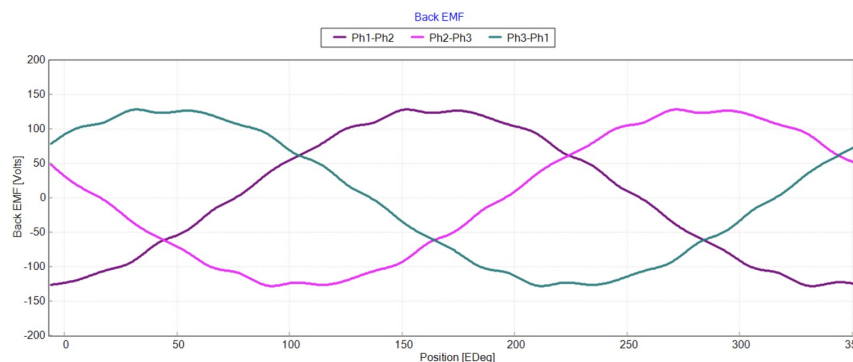

Figure 8. Back EMF Waveform of PMASynRM.

In order to verify the proposed design, FEA is done for the 08-rotor pole structure by selecting the four flux barriers per pole. In this paper, FE results and waveforms are displayed for 08 rotor poles with 04 flux barriers. For both the types of geometries current, voltage and speed are kept constant. FE analysis is done by considering the 150 A current (RMS), 200 V DC bus voltage and 3000 rpm speed. In Table 4 all performance parameters are compared for both the geometries of PMASynRM and PMSM.

In the proposed design of PMASynRM bridges are not provided to get the higher air gap flux density. The bridges in flux rotor structure are significantly affect the torque and power factor of the motor, hence design of rotor rib is very important to achieve target torque with high power factor. For the proposed PMASynRM, due to high number of poles and flux barriers, higher component of magnet flux is produced. Due to higher production of flux, higher back emf is achieved in PMSM.

PMs are placed in the V-shaped, which will concentrate more magnetic field lines during the rotation of rotor. This will help to produce more back emf compared to PMASynRM. Increment in back emf will result in the high output power of the PMSM. Figure 10 and Figure 11 depicts rated electromagnetic torque production of PMASynRM and PMSM respectively. In the PMASynRM, two torque components are present due to reluctance principle and PM interaction with main field flux. Average torque production with the 08-rotor pole and 04-flux barriers is 156 N-m.

For PMASynRM, there is no center rib is kept to increase the torque capability of the motor and also to improve the mechanical integrity of the rotor. In both the motor, torque is produced by the interaction of PMs with the magnetic flux lines generated by the input current to stator winding. In PMSM, to achieve
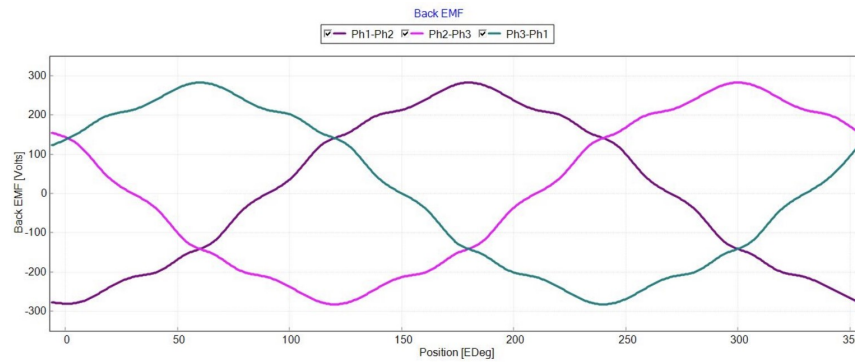
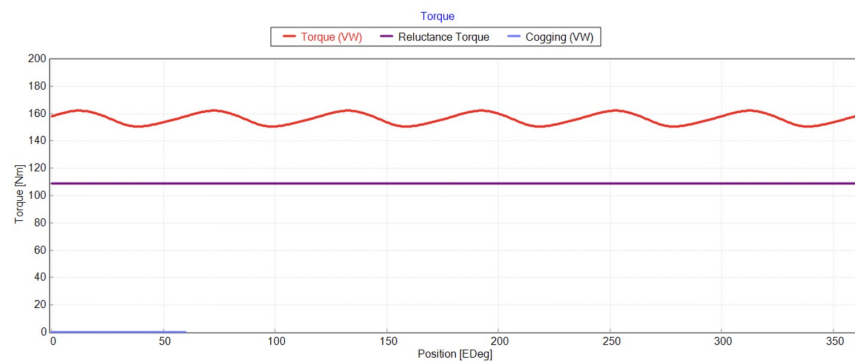**Figure 9.** Back EMF Waveform of PMSM.

Figure 10. Torque Waveform of PMASynRM.

the better air gap flux density, magnets are placed in V-shape near to airgap with higher V-angle. This will help PMs to produce large amount of flux and transfer it towards airgap [14]. This will help the machine to achieve higher flux density in airgap which consequently helps the PMSM to achieve the high torque density.

Similarly, in PMASynRM, a greater number of PMs are placed in barriers, which will help to achieve high airgap flux density. Figure 12 and Figure 13 shows the airgap flux density distribution with respect to the rotor position. In comparison with ferrite magnets, considerably higher power density is achieved in both the motors. Due to present of the magnets, torque ripple is major issue in both the motors. Certain techniques to reduce the torque ripples are implemented and reported in literature for PMASynRM and PMSMs.

To reduce the torque ripples in PMASynRM, by changing the shape of the barriers end is further tilted so barriers face further inward. This will reduce torque ripple at significant level. Value of torque ripple is tabulated in Table 4. For the better control requirements of PMASynRM and PMSM, cogging torque should be as far as reasonably minimum. Cogging torque is oscillating torque in nature. In Figure 14 and Figure 15 cogging torque for PMASymRM and PMSM are represented and it indicates minimum acceptable values.

Flux linkage plays an important role to produce the magnet torque, hence it is necessary to evaluate the flux linkage waveform for both the motors. Rotor core permeance is finite, hence values of flux linkage and inductances will be change with the core saturation. The waveforms are depicted in Figure 16 and Figure 17 and appropriate with respect to the motor performance requirement. Torque-Speed characteristics are illustrated for PMASynRM and PMSM in Figure 18 and Figure 19 for the various phase advance angles.

In Figure 18 and Figure 19, torque speed characteristics is obtained for the various load point advanced angles and it's analyzed that maximum torque envelop was found for load point advance angle 51°. This obtained characteristic found appropriate for the EV motor characteristic. From the figure, it analyzed that PMASynRM offers wide operating range over PMSM with the speed of 3000 rpm. All the required performance parameters are enlisted in Table 4 for both the motor for informal comparative analysis.
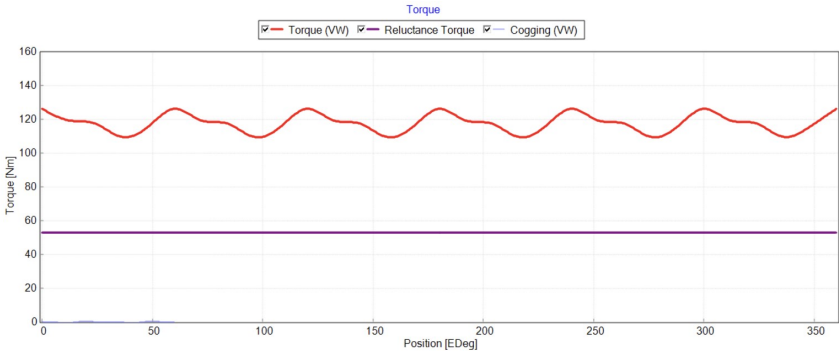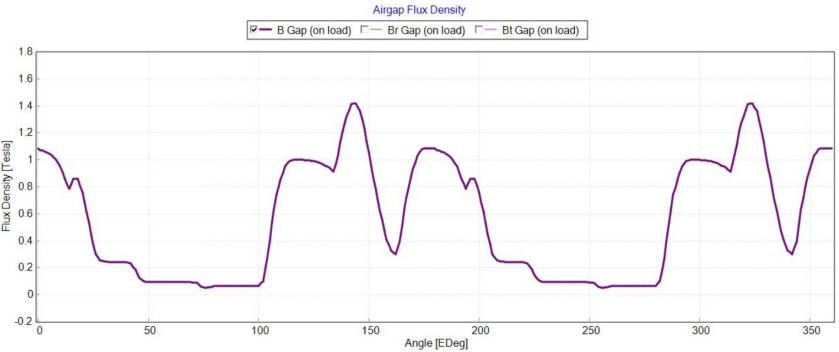
Figure 11. Torque Waveform of PMSM.

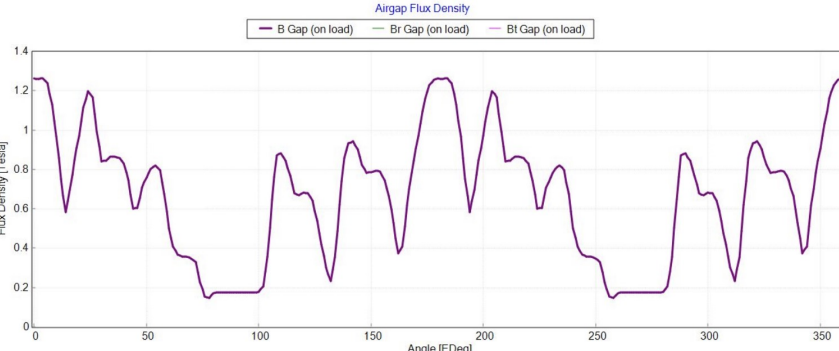**Figure 12.** Airgap flux density Waveform of PMSM.

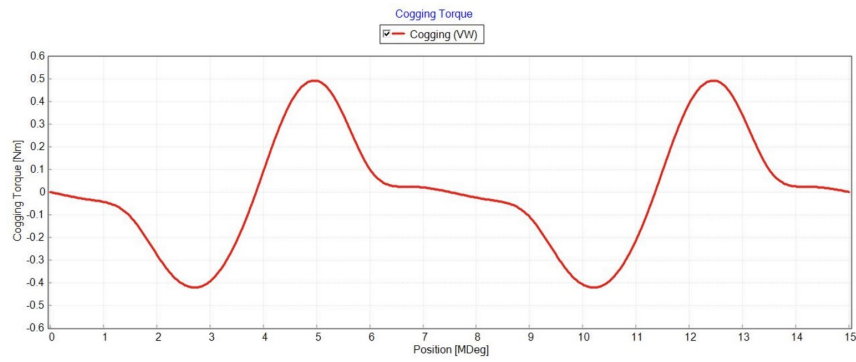**Figure 13.** Airgap flux density Waveform of PMASynRM.

Figure 14. Cogging torque Waveform of PMSM.

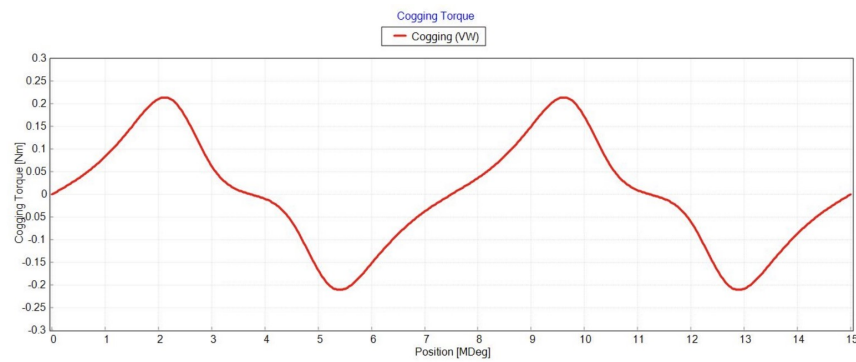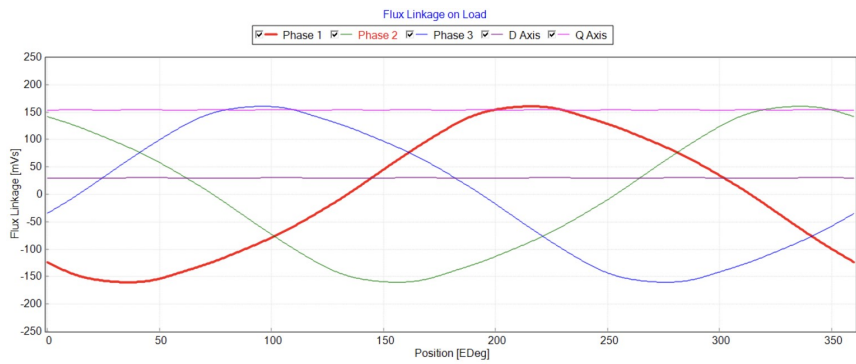**Figure 15.** Cogging torque Waveform of PMASynRM.

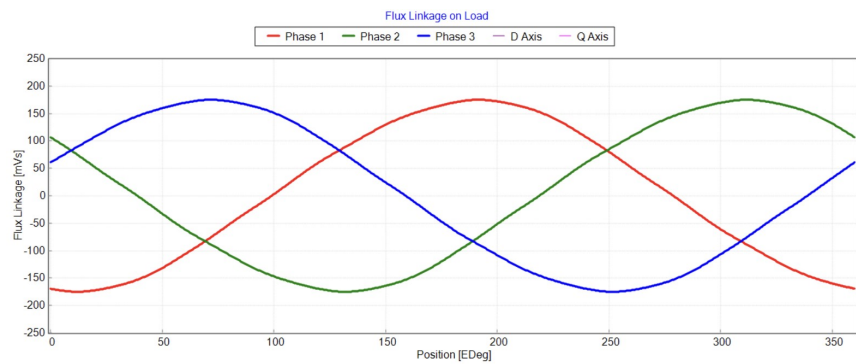**Figure 16.** Flux linkage Waveform (on load) of PMSM.

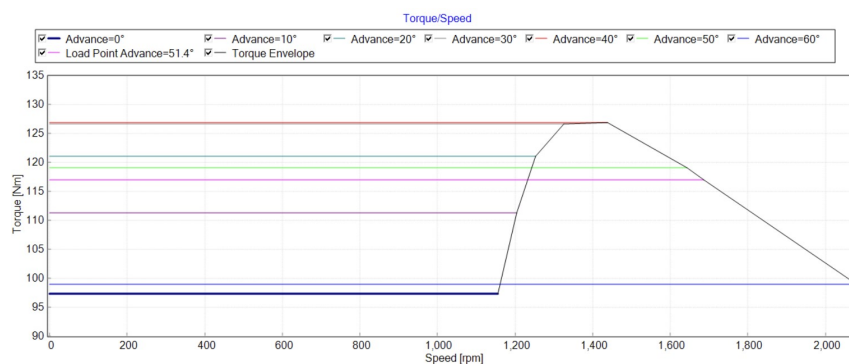**Figure 17.** Flux linkage Waveform (on load) of PMAsynRM.
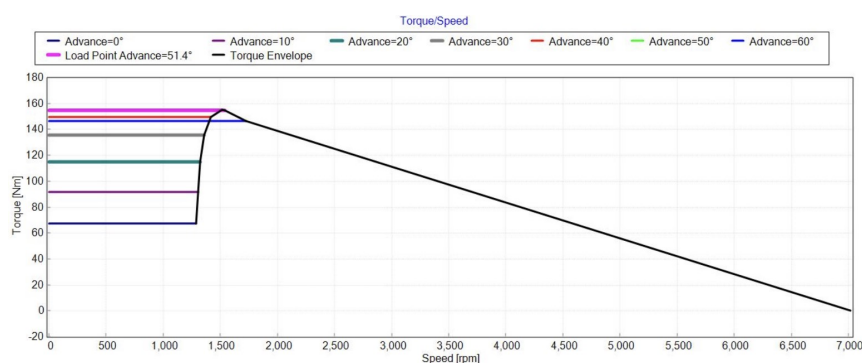
Figure 18. Torque-Speed characteristics of PMSM.

Figure 19. Torque-Speed characteristics of PMASynRM.

Table 4. Comparative analysis of PMASynRM & PMSM.

Performance Parameters	PMASynRM	PMSM
Back EMF (V)	125	187
Air gap Flux density (T)	0.67	0.56
Flux Linkage (mWb)	175	153
Average Torque (N-m)	156	117
PM Torque (N-m)	47	60
Reluctance Torque (N-m)	109	57
Cogging Torque ripple (N-m)	0.21	0.84
Torque Ripple (%)	6.89	13.95
Input Power (kW)	51.37	38.24
Total Losses (kW)	2.9	1.9
Output Power (kW)	48.46	37
Efficiency (%)	94.35	95.13
Power Factor (lagging)	0.73	0.89
d-axis inductance (mH)	0.45	0.82
q-axis inductance (mH)	1.29	1.74
PM Br (T)	1.125	1.125
Number of PMs	32	16
Type of PM	N30UH	N30UH
Current Density (J, A/mm2)	15.16	11.56
Weight (kg)	31.8	35
Torque/volume	92.83	69.88

5. Conclusions

In this paper, performance parameters of V-type PMSM and PMASynRM are compared for EV application. In both the motors, stator winding is kept similar, only change in rotor structure is carried out and performance is investigated. In term of back emf, in PMASynRM back emf depends on the number of poles and magnet flux is comparatively low compared to PMSM. Although the number of poles is more in PMASynRM, but less amount of PM flux interaction is occurred in PMASynRM. Hence back emf component is less compared to PMSM. Based on the FE analysis, 49% more back emf is achieved in PMSM. Due to a higher number of flux barriers in PMASynRM, reluctance torque component is high compared to PMSM. Due to the magnet placement very near to the airgap in PMSM, higher magnet torque is achieved in PMSM, but at the same time due to high reluctance torque in PMAsymRM, electromagnetic torque of PMASynRM (156 N-m) is high compared to PMSM (117 N-m).

Due to the higher volume of PMs in PMASynRM, average air gap flux density achieved is 0.67 T compared to PMSM where the achieved value was 0.56 T. In V-type PMSM due to the placement of magnets near to the airgap, higher torque pulsation is produced which results in the higher torque ripple compared to PMASynRM. In terms of the output power and efficiency, PMASynRM offers higher power compared to the PMSM while offering almost similar efficiency. PMSMs offer improved power factor compared to the PMASynRM due to the higher d-axis inductance. In selection of EV motor, torque/volume ratio is an important parameter for drive cycle. In this work, PMASynRM offers higher torque per volume ratio which is almost 31% higher than the PMSM. In this work, ferrite magnets can be used as a cost-effective solution and to improve other relevant performance parameters.

Author contributions: Swapnil N Jani is involved into development of the main design methodology of proposed work, to carry out the FE simulations through FE software, analyzed and validation of the results. Dr. J. G. Jamnani visualized the study and was in charge of overall direction and planning.

Disclosure statement: The authors declare no conflict of interest.

References

[1] K. Boughrara, R. Ibtiouen, D. Zarko, O. Touhami, and A. Rezzoug. Magnetic field analysis of external rotor permanent-magnet synchronous motors using conformal mapping. *IEEE Transactions on Magnetics*, 46(9):3684–3693, 2010.

[2] J. Bae, S. J. Kim, S. C. Go, H. W. Lee, Y. D. Chun, C. J. Ree, and J. Lee. Novel configuration of the magnetizing fixture for a brushless permanent-magnet motor. *IEEE Transactions on Magnetics*, 45(6):2807–2810, 2009.

[3] V. Rallabandi and B. G. Fernandes. Design procedure of segmented rotor switched reluctance motor for direct drive applications. *IET Electric Power Applications*, 8(3):77–88, 2014.

[4] Z. Q. Zhu and D. Howe. Electrical machines and drives for electric, hybrid, and fuel cell vehicles. *Proceedings of the IEEE*, 95(4):746–765, 2007.

[5] G. Lei, C. Liu, J. Zhu, and Y. Guo. Techniques for multilevel design optimization of permanent magnet motors. *IEEE Transactions on Energy Conversion*, 30(4):1574–1584, 2015.

[6] J. G. Jamnani and S. Jani. Performance analysis of pm assisted synchronous reluctance motor with optimized novel design for electric vehicular application. In *2022 Second International Conference on Sustainable Mobility Applications, Renewables and Technology (SMART)*, pages 1–5. IEEE, 2022.

[7] T. A. Huynh and M. F. Hsieh. Comparative study of pm-assisted synrm and ipmsm on constant power speed range for ev applications. *IEEE Transactions on Magnetics*, 53(11):1–6, 2017.

[8] K. Yamazaki and M. Kumagai. Torque analysis of interior permanent-magnet synchronous motors by considering cross-magnetization: Variation in torque components with permanent-magnet configurations. *IEEE Transactions on Industrial Electronics*, 61(7):3192–3201, 2013.

[9] S. Morimoto. Trend of permanent magnet synchronous machines. *IEEJ Transactions on Electrical and Electronic Engineering*, 2(2):101–108, 2007.

[10] Q. Chen, G. Liu, W. Zhao, L. Sun, M. Shao, and Z. Liu. Design and comparison of two fault-tolerant interior-permanent-magnet motors. *IEEE Transactions on Industrial Electronics*, 61(12):6615–6623, 2014.

[11] C. Zhou, X. Huang, Y. Fang, and L. Wu. Comparison of pmsms with different rotor structures for ev application. In *2018 XIII International Conference on Electrical Machines (ICEM)*, pages 609–614. IEEE, 2018.

[12] E. E. Montalvo-Ortiz, S. N. Foster, J. G. Cintron-Rivera, and E. G. Strangas. Comparison between a spoke-type pmsm and a pmasynrm using ferrite magnets. In *2013 International Electric Machines & Drives Conference*, pages 1080–1087. IEEE, 2013.

[13] W. Zhao, F. Zhao, T. A. Lipo, and B. I. Kwon. Optimal design of a novel v-type interior permanent magnet motor with assisted barriers for the improvement of torque characteristics. *IEEE Transactions on Magnetics*, 50(11):1–4, 2014.

[14] G. Liu, G. Xu, W. Zhao, X. Du, and Q. Chen. Improvement of torque capability of permanent-magnet motor by using hybrid rotor configuration. *IEEE Transactions on Energy Conversion*, 32(3):953–962, 2017.

[15] T. A. Huynh and M. F. Hsieh. Performance analysis of permanent magnet motors for electric vehicles (ev) traction considering driving cycles. *Energies*, 11(6):1385, 2018.

[16] C. C. C. dos Santos, J. L. R. Ortiz, J. P. Américo, and K. S. C. Linares. Nonlinear modeling of magnetic materials for electromagnetic devices simulation. In *2017 IEEE XXIV International Conference on Electronics, Electrical Engineering and Computing (INTERCON)*, pages 1–4. IEEE, 2017.

[17] M. Dośpiał, M. Nabiałek, M. Szota, P. Pietrusiewicz, K. Gruszka, and K. Błoch. Modeling the hysteresis loop in hard magnetic materials using t (x) model. *Acta Physica Polonica A*, 126(1):170–171, 2014.

[18] K. Jacques, F. Henrotte, J. Gyselinck, R. Sabariego, and C. Geuzaine. Comparison between the energy-based hysteresis model and the jiles-atherton model in finite element simulations. In *International Symposium on Applied Electromagnetics*, 2017.

[19] Nihat Ozturk, Adem Dalcali, Emre Celik, and Selcuk Sakar. Cogging torque reduction by optimal design of pm synchronous generator for wind turbines. *International Journal of Hydrogen Energy*, 42(28):17593–17600, 2017.

[20] Adem Dalcalı, Erol Kurt, Emre Çelik, and Nihat Ozturk. Cogging torque minimization using skewed and separated magnet geometries. *Politeknik Dergisi*, 2020.

[21] Erdal Bekiroglu and Sadullah Esmer. Design and double-stage optimization of synchronous reluctance motor for electric vehicles. *RS Communications*, 2022.

[22] C. E. M. İ. L. Ocak, A. Dalcalı, E. M. R. E. Çelik, and Durmuş Uygun. Fea-based design improvement of small scale bldcms considering magnet thickness and pole embrace. *Int'l Journal of Computing, Communications & Instrumentation Engg*, 4(2):31–35, 2017.

[23] Ali Saygın, Cemil Ocak, Adem Dalcalı, and Emre Çelik. Optimum rotor design of small pm bldc motor based on high efficiency criteria. *ARPN Journal of Engineering and Applied Sciences*, 10(19):9127–9132, 2015.

[24] S. N. Jani and J. G. Jamnani. Performance analysis and comparison of pm-assisted synchronous reluctance motor with ferrites and rare-earth magnet materials. *Materials Today: Proceedings*, 62:7162–7167, 2022.